Ion Thruster Technology Applied to a 30-cm Multipole Sputtering Ion Source

Raymond S. Robinson* and Harold R. Kaufman†
Colorado State University, Fort Collins, Colo.

A 30-cm electron bombardment ion source has been designed and fabricated for micromachining and sputtering applications. This source has a multipole magnetic field that employs permanent magnets between permeable pole pieces. An average ion current density of 1 mA/cm^2 with 500 eV argon ions was selected as a design operating condition. The ion beam at this operating condition was uniform and well collimated, with an average variation of ±5% over the center 20 cm of the beam at a distance up to 30 cm from the ion source.

Introduction

An ion source with a multipole magnetic field is reported by Isaacson and Kaufman.[1] As described therein, this design is conceptually related to both the multipole approach of Moore[2] and Ramsey,[3] and the cusped field approach of Beattie and Wilbur.[4] The major departures herein from the design as reported by Isaacson and Kaufman were the use of permanent magnets in place of electromagnets and the doubling of the discharge chamber diameter.

The performance objectives for sputtering and ion machining applications are high ion current density and a uniform beam profile. Argon is the usual propellant and an ion energy of 500 eV gives a good compromise between material removal and heating and/or damage to the substrate. Wider application of ion machining as a production technique will require larger ion sources. The 30-cm beam diameter used herein represents a substantial increases over previous sources used in these applications. It is also the largest ion beam that can be conveniently generated in the widely available 45 cm size bell jar. The design condition selected for this 30 cm ion source was 1 mA/cm^2 of 500 eV argon ions. The beam should also be uniform and collimated so that a high ion current density can be used at a large distance from the ion source. An increased distance from the source to the target, of course, decreases mutual contamination of the target and the ion source.

Ion Source Design

Discharge Chamber

A cylindrical discharge chamber was selected with a diameter of 30 cm and a depth of 10 cm, as indicated in Fig. 1. A multipole discharge chamber will generally produce a more uniform beam as it is decreased in depth, but the minimum gas pressure required for operation will also increase as the depth is decreased. Data obtained by Isaacson and Kaufman[1] showed these trends down to a depth equal to about half the 15 cm diameter used in their investigations. The absence of any further improvement in uniformity for smaller depths was felt due, in part, to the close proximity of the central cathode and the accelerator system. With the circumferential cathode employed herein, a further decrease in depth was expected to improve the beam uniformity. A depth equal to a third of the 30 cm diameter was therefore selected.

A 30 cm discharge chamber diameter, together with anodes, pole pieces, and other required hardware, results in an overall source diameter of about 42 cm. Thus a 30 cm ion beam is about the largest that can conveniently be used with the entire source still fitting in a 45 cm diameter bell jar.

The pole pieces in the 30 cm source were fabricated of 1.5 mm thick low carbon steel. They were about 2.5 cm deep and spaced about 2.5 cm apart. The magnetic field was provided by 139 Alnic V permanent magnets that were 6 mm in diameter and 2.4 cm long. The sense of the magnets was such that the magnetic polarity of adjacent pole pieces was opposite. The fringe field falls off rapidly with increasing distance from pole pieces, so that the magnetic field was negligible over most of the discharge chamber volume. This resulted in free access of this volume by primary electrons, which would be expected to give a uniform plasma density.

Ten 1.5 mm thick stainless steel anodes were located at equal spacings along the side and back of the discharge chamber, with each anode midway between the two neighboring pole pieces (see Fig. 1). The six back anodes were cylinders, ranging from 2.5 to 28 cm in diameter. The four side anodes were flat annular shapes with an inside diameter of about 30 cm. (The two corner anodes were recessed, as discussed in the following section. As a result of this recessing, one of the four side anodes had an inside diameter of 30.5 cm.)

Required Magnetic Field Strength

A fringe magnetic field adjacent to multipole anodes prevents the escape of primary electrons before most of their energy is expended in the production of ions. In calculating the deflection of an electron in such a fringe field, it is assumed that the radius of curvature of the anode is large compared to the depth of fringe field. It is further assumed that the magnetic induction $\boldsymbol{B}$ is parallel to the anode and that its magnitude varies only as a function of distance x from the anode.

In passing through an infinitesimal region dx, an electron with a component of velocity v normal to $\boldsymbol{B}$ is deflected through an angle $d\theta$, as indicated in Fig. 2. The radius of curvature of the electron path in the region dx is $r = mv/qB(x)$, where m and q are the mass and charge of an electron. The radius r can be related to $d\theta$ and dx through geometrical considerations, $r\,d\theta = dx/\sin\theta$. Combining the last two expressions to eliminate r, $B(x)\,dx = (mv/q)\,\sin\theta\,d\theta$. The integral of $B(x)\,dx$ can be related to the electron deflection by

$$\int_0^D B(x)\,dx = \int_{\theta_i}^{\theta_f} (mv/q)\sin\theta\,d\theta$$

where θ_i is the incident electron angle and θ_f is the angle after an electron traverses a thickness D of magnetic induction. The

Presented as Paper 76-1016 at the AIAA International Electric Propulsion Conference, Key Biscayne, Fla., Nov. 14-17, 1976; submitted Dec. 13, 1976; revision received Feb. 28, 1977.

Index categories: Aerospace Technology Utilization; Electric and Advanced Space Propulsion.

*Research Associate, Dept. of Physics. Member AIAA.

†Professor, Dept. of Physics. Associate Fellow AIAA.

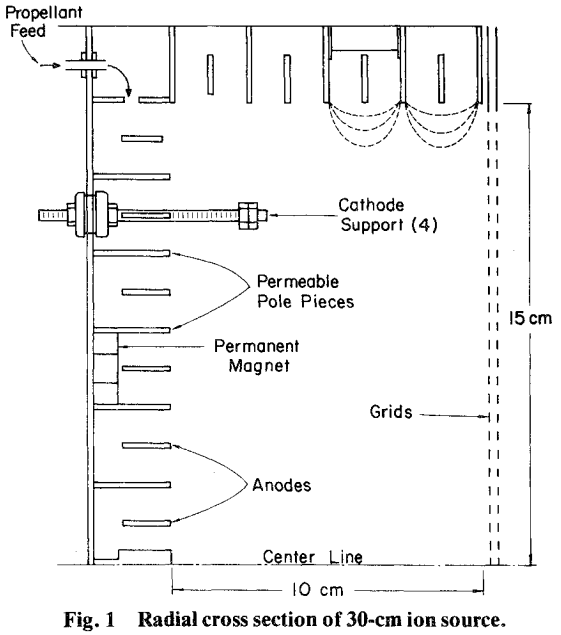

Fig. 1 Radial cross section of 30-cm ion source.

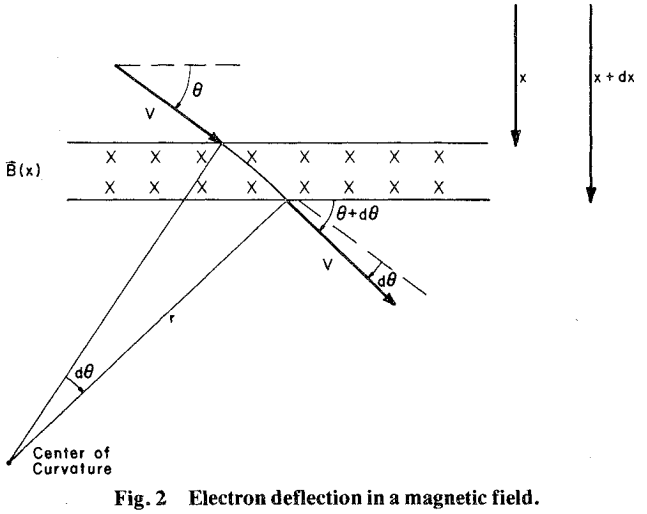

Fig. 2 Electron deflection in a magnetic field.

maximum value of the angular integral corresponds to the maximum electron penetration toward the anode, and is obtained with θ_i equal to zero and θ_f equal to π. For these limits,

$$\int_0^D B(x)\,dx = 2mv/q$$

In terms of electron kinetic energy E,

$$\int_0^D B(x)\,dx = (8mE/q^2)^{1/2}$$

With the substitution for electron charge and mass, this becomes

$$\int_0^D B(x)\,dx = 6.74\times 10^{-6}E^{1/2}$$

where E is in electron-volts and the left-hand side is in SI units. This expression provides a criterion on the integrated magnetic field for primary electron containment.

For 50 eV primary electrons, an integrated magnetic field of 48 gauss-cm is indicated by the preceding equation. To allow for several factors not included in this simple derivation, the

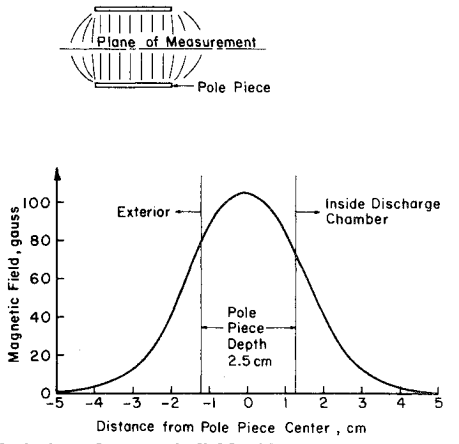

Fig. 3 Variation of magnetic field midway between two pole pieces.

30 cm source was designed for an integrated field approximately 50% larger than this value.

Figure 3 shows a typical variation of magnetic field strength midway between two permeable pole pieces. The magnetic field was numerically integrated from the inner edge of an anode out to the nearly field-free region in the discharge chamber. In most cases the inner edge of the anode was flush with the inner edges of the two neighboring pole pieces. The two corner anodes, however, were recessed 2.5 mm behind neighboring pole pieces. The recessing of corner anodes had been found earlier to be a convenient solution to the corner problem of the multipole discharge chamber.[1] The 2.5 mm recess used herein resulted in an increase of about 18 gauss-cm for the field integrals over the corner anodes. Without this increase, the integrals for the corner anodes would have been substantially smaller than the integrals for other anodes.

The magnetic field integrals over the 10 anodes are shown in Fig. 4. The average is about 77 gauss-cm, while the minimum is about 67 gauss-cm at anode number 7 (a corner anode). The placement of the permanent magnets was selected to give uniformity of the magnetic field and the integral of this field (Fig. 4), While adequate uniformity was obtained with uniform spacing of the side magnets, the back (upstream) magnets required more of a trial and error approach. The final arrangement for these back magnets is shown in Fig. 5. Note that magnets in neighboring sections were staggered to avoid local saturation of pole pieces. The magnets in the side sections were also staggered, although in a more regular manner.

Cathodes

Refractory metal cathodes of 0.25 mm tantalum wire were used for both the discharge chamber and the neutralizer. The periodic maintenance of refractory wire cathodes is not a

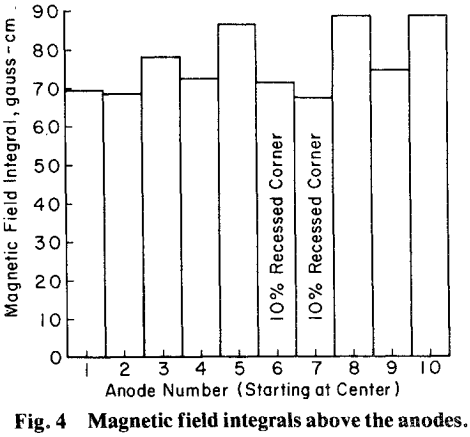

Fig. 4 Magnetic field integrals above the anodes.

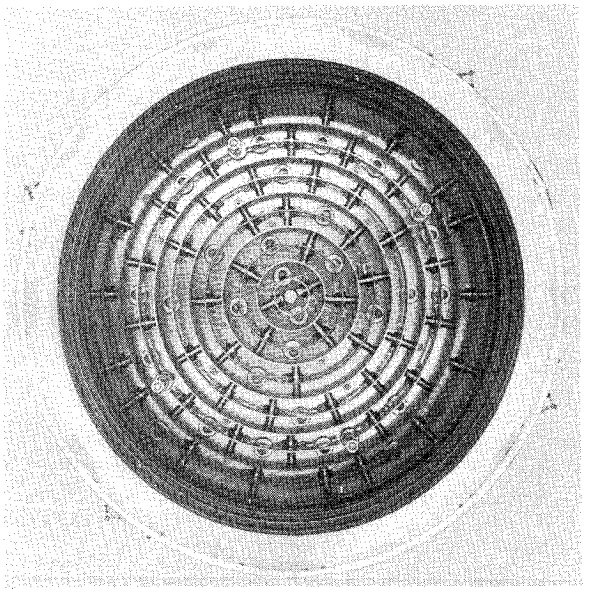

Fig. 5 Back (upstream end) of 30-cm discharge chamber (inside view).

major problem in ground applications. On the other hand, the extended emission surface of a wire discharge chamber cathode can be a definite advantage in obtaining a uniform beam profile. Tungsten wire could have been used instead, but tantalum was preferred because of its greater ductility.

The discharge chamber cathode was in the shape of a square, held at the corners by four supports extending through the back wall of the discharge chamber (Fig. 1). Electrical connections were made so that the four cathode sections were effectively in parallel. Cathode placement was selected to enhance beam uniformity. The cathode was near the side (cylindrical) wall of the discharge chamber to offset the decrease in plasma density usually found in that location. It was also located nearer the upstream end of the chamber to permit the use of a very flat chamber without the sharp peaks that are found when a cathode is close to the accelerator system.

The neutralizer cathode was one strand of tantalum stretched across the beam about 5 cm from the accelerator system. Neutralization was obtained with an ion beam by increasing the heating current until no net current was measured to a grounded probe located in the center of the beam.

Both the discharge chamber cathode and the neutralizer cathode were heated with 60 Hz current. The center tap of the discharge chamber heater winding was at the potential of the discharge chamber outer shell. The neutralizer heater center tap was grounded.

Accelerator System

Two accelerator systems were tested with the 30 cm ion source. One system used flat carbon grids, while the other used dished molybdenum grids.

Flat Carbon Grids—the carbon grids were fabricated from dense, fine grained carbon (Union Carbide, Grade ATJ). The holes were drilled in a close packed hexagonal pattern with 4.1 mm between centers. The screen holes were 3.3 mm in diameter (57% open area), while the accelerator holes were 2.6 mm in diameter. Both grids were 1.5 mm thick, but the beam area of the screen (30 cm diameter) was milled down to a thickness of 0.76 mm.

Ion optics data from Aston and Kaufman[5] were used to determine the optimum spacing between grids. For minimum beam divergence at 1 mA/cm^2, this spacing was calculated at 1.7 mm for the carbon grid geometry. Grid elasticity, however, was found to be a problem. In the usual horizontal grid position (ion beam directed downwards), the screen was found to sag 1 mm closer to the accelerator in the center than at the edge of the beam. Further, with the screen 50°C hotter than the accelerator, thermal expansion would account for the rest of the 1.7 mm spacing. Experimentally, severe high voltage arcing was encountered in the center of the grids after a short operating time. Because of these limitations, a separation of 2.5 mm was used for the carbon grids.

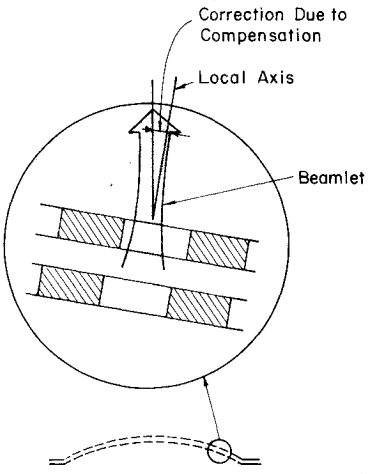

Fig. 6 Deflection of beamlet toward axial direction by compensated grids.

Dished Molybdenum Grids—a set of dished molybdenum grids was supplied by the NASA Lewis Research Center. The screen was fabricated of 0.38 mm thick molybdenum with 1.9 mm holes on 2.2 mm centers (67% open area). The accelerator was 0.51 mm thick, with 1.6 mm holes. The grids were dished outwards from the discharge chamber, with a dishing depth of about 2.5 cm. The hole pattern lies within a 28 cm diameter for these grids.

Because of the dishing, the ion beam would be strongly divergent if the spacing between holes were the same for both grids. To deflect the beamlets back toward the axial direction, the grids are compensated, that is, the spacing between holes is made slightly larger in the accelerator grid. The resulting hole displacement and beamlet deflection is indicated in Fig. 6.

Using the same ion optics data,[5] a grid separation of 1.7 mm was also indicated for minimum beam divergence at 1 mA/cm^2 with the dished molybdenum grids. The accelerator system functioned well at this spacing. It also functioned well at a reduced spacing of 0.84 mm, with no visual or operational indications that this spacing was too close.

Experimental Results

The ion source was operated in a 1.2 m diameter vacuum chamber, which could be pumped down to 3×10^{-6} torr in the absence of argon flow. The discharge was initiated by increasing the argon flow to a high value, high enough to cause severe arcing if the high voltage was applied without reducing the argon flow. Starting procedure also included increasing the discharge from the normal 50V to 62V and temporarily increasing the ion source shell to anode potential. Both of these tended to increase the initial space-charge-limited electron emission. Normal operation was at both 900 mA-equivalent argon flow (about 1×10^{-5} torr facility pressure) and 1500 mA-equivalent (about 1.5×10^{-5} torr). Attempts to maintain a discharge while lowering the argon flow rate to 600 mA-equivalent were not successful.

Discharge Chamber Performance

The discharge chamber data shown in Fig. 7 are typical for the two accelerator systems tested. Both sets of grids were operated at the same screen and accelerator voltages and, for

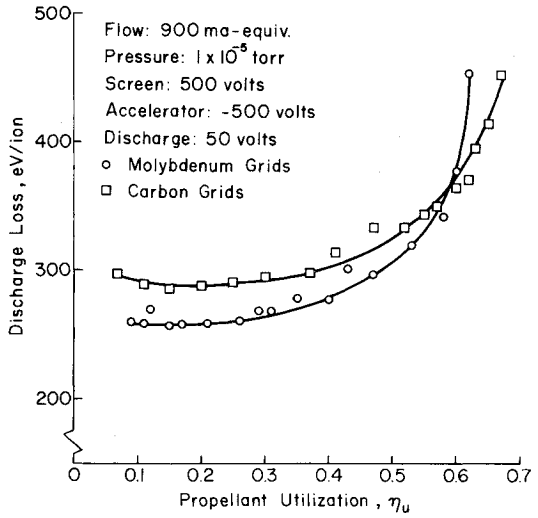

Fig. 7 Discharge chamber performance.

this comparison, at the same separation distance (1.7mm). This discharge voltage was maintained at a constant 50V for both performance tests. Discharge current for the carbon grid test was varied from 0.4A to 6.5A while the beam current increased from 60mA to 610mA. Discharge current for the molybdenum grid test was varied from 0.4A to 5.1A while the beam current increased from 80mA to 560mA. The total power necessary to operate the source with a 430mA beam of 500eV ions including cathode heater and beam powers is approximately 820W.

Lower discharge losses were obtained with the molybdenum grids over most of the operating range, which was attributed to the larger open area fraction of that screen grid. On the other hand, slightly higher propellant utilization could be obtained with the carbon grids, which was attributed to the smaller open area fraction of that accelerator grid.

Although the propellant utilization shown in Fig. 7 was uncorrected for both double ionization and propellant backflow from the facility, estimates were made of the relative magnitude of these parameters.

The ratio of double ion current to single ion current in the source efflux was estimated by comparison with data from a multipole argon ion source with the same discharge chamber depth as the 30-cm ion source but with a diameter half as large.[1] Allowing for an increase in double ion production as the primary electron region volume to surface area ratio increases for the larger chamber, an estimate of approximately 0.02 for the ratio of double ion current to single ion current was calculated. This would imply a reduction in the quoted propellant utilizations of only about 0.01. In sputtering applications double ions would strike the substrate with twice the energy of single ions. It may be necessary in some applications to take this maximum energy into account.

Backflow of propellant through the grids was estimated from free molecular flow calculations. For the ambient pressure condition of Fig. 7 the backflow was estimated at 85mA-equivalent through the carbon grids and 115mA-equivalent through the molybdenum grids. Correcting for backflow would reduce the quoted propellant utilizations by 9% for the carbon grid test and 11% for the molybdenum grid test. These corrections are of nearly the same magnitude so that the qualitative results shown in Fig. 7 are unchanged. Even with allowances for these corrections, the attainable utilizations appear reasonable for ground applications. The level of discharge losses is quite low for ground applications and quite impressive considering that no changes were necessary in the discharge chamber to reach this performance level.

Ion Beam Profiles

The current density in the ion beam was measured with Faraday probes. The current collecting surfaces were 6.4-mm diameter disks of molybdenum. These disks were located flush with a surrounding ground shield and biased at −25V relative to ground to reflect electrons.

The effect of varying the distance between the probe and the ion source is shown in Fig. 8. The current density in the center of the beam is attenuated about 25% as the distance is increased from 10 to 30 cm. This attenuation is believed to result primarily from ion interactions with the ambient gas in the vacuum facility, together with the local contribution due to neutrals that escape from the ion source. Some attenuation in current density is probably also the result of beam divergence, although beam divergence appears small in the 10 to 30 cm range.

Ion-beam profiles 10 cm from the carbon and molybdenum grids are shown in Figs. 9 and 10 for several combinations of screen and accelerator grid potential. The ion beam current was set for each potential combination by: 1) reaching the maximum beam current for that propellant flow rate; or 2) encountering a rapid increase in impingement with increasing beam current, then decreasing the beam current until the impingement returned to normal and stable operation was observed.

Because of the larger than optimum spacing used for the carbon grids, increasing the total voltage between grids gives a substantial increase in the allowable beam current and current density. In contrast, the molybdenum grids were set near optimum spacing for 500 eV ions—and probably were somewhat closer at operating temperature. As a result, higher voltages give a slight reduction in beam current, possibly due to excessive cross-over of ion trajectories.

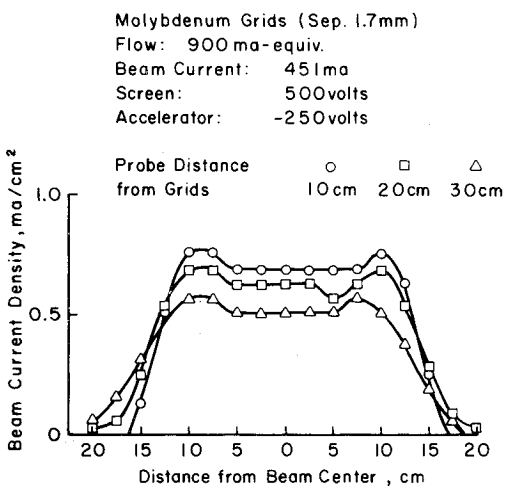

Fig. 8 Variation of ion-beam profile with distance from ion source.

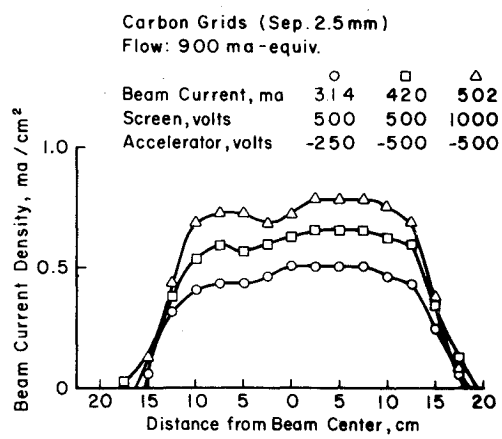

Fig. 9 Ion-beam profiles for carbon grids with 900 mA-equivalent argon flow.

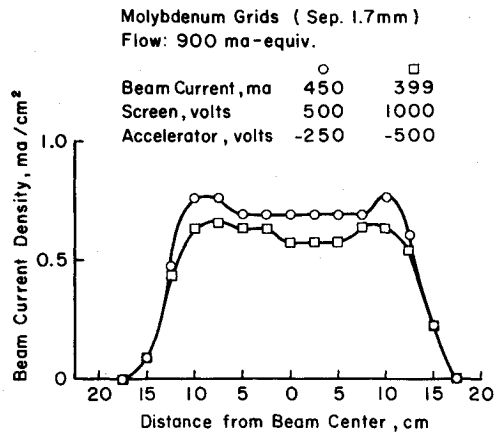

Fig. 10 Ion-beam profiles for molybdenum grids with 900 mA-equivalent argon flow.

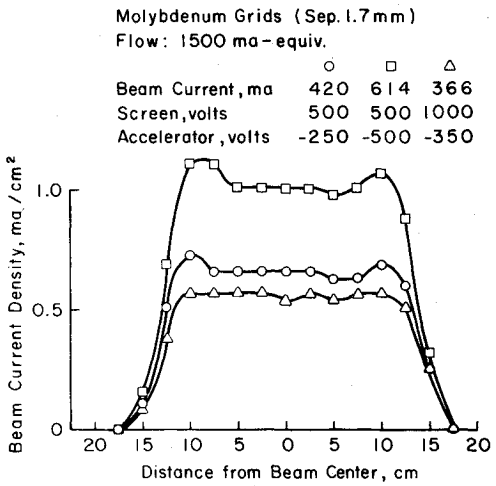

Fig. 11 Ion-beam profiles for molybdenum grids with 1500 mA-equivalent argon flow.

The difference in profile shape for the two grid sets is felt to be significant. The carbon grids gave slightly rounded profiles. (The slight asymmetry also shown could be due to a similar asymmetry in either electron emission in the discharge chamber or the gap between the grids. Regardless of the cause, this asymmetry is not important to the following discussion.) The carbon grids are known to be closer together in the center of the beam, so that the plasma density in the discharge chamber should be slightly more uniform than the profiles shown in Fig. 9.

The profiles for the molybdenum grids are interesting in that they show peaks near the outer edge of the ion beam. If these peaks reflected the variation in discharge-chamber plasma density, then they should have also been evident with carbon grids. The peaks shown in Figs. 8 and 10 are believed to result from the dished shape of the molybdenum grids, although the specific process is not clear. For example, the spacing between dished grids is known to vary across the beam diameter at operating temperatures.[6] Despite this variation, the relative displacement of screen and accelerator holes to deflect the beamlets in the axial direction was made a linear function of distance from the beam center. This discrepancy would be expected to produce some ion-optic aberration. Another possible cause of the peaks is in the deceleration region downstream of the accelerator. The decelerating electric field is nearly normal to the local dished grid surface, but the ion trajectories are at an appreciable angle to this normal near the edge of the beam. The relative directions of electric field and trajectories could therefore cause further deflections near the edge of the beam; which could cause the observed peaks.

The maximum current densities in Figs. 9 and 10 differ by only about 10% and are therefore probably determined by the production rate of ions in the discharge chamber. Data were taken at a higher propellant flow rate in an attempt to increase maximum current density. As shown in Fig. 11, a current density of 1 mA/cm^2 was obtained with a flow rate of 1500 mA-equivalent and grid potentials of 500V and 500V. As was also shown in Fig. 10, a substantial increase in total voltage leads to a decrease in beam current, not an increase.

Although data for the 1500 mA-equivalent flow rate are not shown for the carbon grids, a current density of about 1.0 mA/cm^2 was obtained at 1000V and 500V. Essentially no improvement was obtained over the 900 mA-equivalent flow at lower voltages.

Concluding Remarks

The multipole magnetic field used in the 30 cm ion source resulted in low discharge losses and a uniform ion beam. The flat carbon grids permitted current densities up to 1 mA/cm^2, but at 1000 eV argon ion energy. The dished molybdenum grids permitted the design current density of 1 mA/cm^2 at the design argon ion energy of 500 eV. The difference in performance for these two accelerator systems is attributed, for the most part, to the larger spacing required for the carbon grids.

The uniformity was typically within ±5% over the center 20 cm of the beam with the dished molybdenum grids. The uniformity for the flat carbon grids was poorer, averaging ±8% for the center 20 cm of the beam.

Of particular interest was the absence of any development iterations in the multipole discharge chamber design. The procedure followed can apparently give a uniform profile and low discharge losses without the usual trial and error development.

Acknowledgment

This research was supported by NASA Grant NSG-3086.

References

[1]Isaacson, G. C. and Kaufman, H. R., "15-cm Multipole Gas Ion Thruster," AIAA Paper 76-1045, Key Biscayne, Fla., 1976; submitted to *Journal of Spacecraft and Rockets*.

[2]Moore, R. D., "Magnetoelectrostatically Contained Plasma Ion Thruster," AIAA Paper 69-260, Williamsburg, Va., 1969.

[3]Ramsey, W. D., "12-cm Magneto-Electrostatic Containment Mercury Ion Thruster Development," *Journal of Spacecraft and Rockets*, Vol. 9, May 1972, pp. 318-321.

[4]Beattie, J. R. and Wilbur, P. J., "Cusped Magnetic Field Mercury Ion Thruster," AIAA Paper 76-1011, Key Biscayne, Fla., 1976; submitted to *Journal of Spacecraft and Rockets*.

[5]Aston, G. and Kaufman, H. R., "Ion Optics of a Two-Grid Electron-Bombardment Thruster," AIAA Paper 76-1029, Key Biscayne, Fla., 1976.

[6]Rawlin, V. K., Banks, B. A., and Byers, D. C., "Dished Accelerator Grids on a 30-cm Ion Thruster," *Journal of Spacecraft and Rockets*, Vol. 10, Jan. 1973, pp. 29-35.